Syntheses, Structures, and Characterization of the Two-Dimensional Tellurides $CsCu_2MTe_4$ (M = Nb, Ta)

Jason A. Cody, Eric J. Wu, Chi M. Cheung, and James A. Ibers

Department of Chemistry, Northwestern University, Evanston, Illinois 60208-3113

The new compounds $CsCu_2MTe_4$ (M = Nb, Ta) have been synthesized at 900°C through the reaction of Cu and Nb or Ta with a Cs_2Te_3/Te melt as a reactive flux. Single-crystal X-ray diffraction measurements show that both compounds crystallize in the space group $Pn2_1a$ of the orthorhombic system with four formula units in cells of dimensions a = 8.198(2) Å, b = 5.988(2) Å, c = 20.527(6) Å, V = 1007.7(6) Å³ at 113 K for M = Nb, and a = 8.217(5) Å, b = 5.992(5) Å, c = 20.562(14) Å, V = 1012(1) Å³ at 113 K for M = Ta. The two compounds are isostructural. The structure of $CsCu_2NbTe_4$ comprises infinite, two-dimensional layers of Cu- and Nb-centered tetrahedra; Cs^+ cations separate the layers. Each Cs^+ cation is coordinated by nine Te atoms at the corners of a highly distorted tricapped trigonal prism. Both phases are highly resistive. © 1996 Academic Press, Inc.

INTRODUCTION

The compounds K_3MQ_4 (M = Nb, Ta) (1), $K_2CuNbSe_4$ (2), $K_2CuTaSe_4$ (3), KCu_2NbQ_4 (Q = S, Se) (4), KCu_2TaSe_4 (5, 6), and Cu_3NbSe_4 (5) were previously synthesized and characterized in this laboratory. Sequential substitution of Cu^+ for K^+ ions results in an increase in the dimensionality of the structures (7), from the packing of isolated K^+ and MQ_4^{3-} ions in K_3MQ_4 to infinite one-dimensional metal–chalcogen chains in K_2CuMQ_4 to two-dimensional metal–chalcogen layers in KCu_2MQ_4 to the infinite three-dimensional covalent network in Cu_3NbSe_4.

In a related series of compounds $ACuMQ_3$ (A = Na, K; M = Ti, Zr, Hf; Q = S, Se, Te) layered structures for the compounds with A = Na (8) differ from those with A = K (9) except for the anomalous compound $NaCuZrS_3$ which exhibits the structure of the A = K series. This result prompted us to look for compounds with A = Cs. We found no quaternary compounds, but rather the ternary compound $Cs_4Zr_3Te_{16}$ (10). The structure of this compound, although similar to that of $K_4M_3Te_{17}$ (M = Zr, Hf) (11), shows different stoichiometry and bonding within the M/Te chains.

Returning to the Nb and Ta series, we find that quater-

nary compounds can be made with Cs. Here we present the syntheses and characterization of the new compounds $CsCu_2MTe_4$ (M = Nb, Ta). Whereas their structures comprise layers similar to those found in KCu_2NbSe_4, the layers are arranged differently.

EXPERIMENTAL

Synthesis

Cs_2Te_3 was synthesized at −79°C from the reaction of stoichiometric amounts of elemental Cs (Aldrich, 99.5%) and Te in liquid ammonia under an Ar atmosphere. Single crystals of $CsCu_2NbTe_4$ were synthesized from a reaction of Cs_2Te_3 (206 mg, 0.32 mmole) with elemental Cu (8 mg, 0.13 mmole; ALFA, 99.5%), Nb (11 mg, 0.13 mmole; Aldrich, 99.9%), and Te (24 mg, 0.19 mmole; Aldrich, 99.8%). $CsCu_2TaTe_4$ was synthesized from a reaction of Cs_2Te_3 (76 mg, 0.12 mmole) with elemental Cu (15 mg, 0.23 mmole), Ta (85 mg, 0.47 mmole; Aldrich, 99.9%), and Te (75 mg, 0.58 mmole). The reaction mixtures were loaded into fused silica tubes in a dry box under an Ar atmosphere; the tubes were evacuated to ∼10^{-4} Torr and sealed. The samples that contained Nb were heated in a furnace at 650°C for 1 day, and then 900°C for 5 days before being cooled at 3°C/hr to room temperature; the samples that contained Ta were heated at 600°C for 1 day and then 900°C for 8 days before being cooled at 3°C/hr to room temperature. The resultant air-stable, lustrous crystals were manually extracted from the solidified melts. Analysis of several crystals with an EDX-equipped Hitachi S-570 scanning electron microscope gave the approximate ratios Cs : Cu : Nb : Te = 2 : 2 : 1 : 4 and Cs : Cu : Ta : Te = 2 : 2 : 2 : 4.

Electrical Conductivity

Single crystals of $CsCu_2NbTe_4$ and $CsCu_2TaTe_4$ ranging in length from 0.6 to 1.5 mm were mounted with Ag paint on Au wires with graphite extensions. Two-probe dc resistivity measurements along the needle axes [010] were made at room temperature.

TABLE 1
Crystal Data and Intensity Collection Details for CsCu$_2$MTe$_4$ (M = Nb, Ta)

	CsCu$_2$NbTe$_4$	CsCu$_2$TaTe$_4$
Formula	CsCu$_2$NbTe$_4$	CsCu$_2$TaTe$_4$
Formula mass (amu)	863.30	951.34
Space group	C_{2v}^9-$Pn2_1a$	$Pn2_1a$
a (Å)	8.198(2)[a]	8.217(5)[a]
b (Å)	5.988(2)	5.992(5)
c (Å)	20.527(6)	20.562(14)
V (Å^3)	1007.7(6)	1012.4(13)
Z	4	4
ρ_c (g cm^{-3})	5.691	6.241
T of data collection (K)[b]	113(2)	113(2)
Crystal shape	Rectangular needle (0.37 × 0.07 × 0.03 mm) bounded by {100}, {010}, {001}	Rectangular needle (0.42 × 0.02 × 0.01 mm) bounded by {100}, {010}, {001}
Crystal volume (mm^3)	7.5 × 10^{-4}	8.4 × 10^{-5}
Radiation	λ(MoKα_1) = 0.7093	λ(MoKα_1) = 0.7093
Linear absorption coefficient (cm^{-1})	201	297
Transmission factors[c]	0.253–0.552	0.590–0.749
Secondary extinction coefficient	0.00152(7)	0.00092(13)
Detector aperture (mm)	6.5 × 6.5, 32 cm from crystal	6.5 × 6.5, 32 cm from crystal
Scan type	$\theta - 2\theta$	$\theta - 2\theta$
Scan speed (deg min^{-1})	2	2
Scan range (deg)	−1.2 to +0.9	−0.9 to +0.6
Takeoff angle (deg)	2.5	2.5
θ limits (deg)	2.67 ≤ θ ≤ 30.72	2.66 ≤ θ ≤ 30.49
Background counts[d]	10 sec at each end of scan	10 sec at each end of scan
Weighting scheme	$w^{-1} = \sigma^2(F_o^2) + (0.04 \times F_o^2)^2$	$w^{-1} = \sigma^2(F_o^2) + (0.04 \times F_o^2)^2$
Data collected	±h, ±k, ±l	−h, ±k, ±l
No. of data collected	11915	6415
No. of unique data, including 0 ≥ F_o^2 ≥ −3σ(F_o^2)	3121	3113
$R_{average}$	0.0529	0.1535
No. of variables	74	74
R_w(F^2) (all data)	0.0782	0.2313
R(on F for $F_o^2 >$ 2σ(F_o^2),	0.0362	0.1015
Error in observation of unit weight (e^2)	1.001	1.419
Absolute structure parameter	−0.01(3)	−0.02(5)

[a] Obtained from a refinement with the constraints $\alpha = \beta = \gamma = 90°$.
[b] The low-temperature system is based on a design by Huffman (12).
[c] The analytical method, as employed in the Northwestern absorption program AGNOST, was used for the absorption correction (17).
[d] The diffractometer was operated with the use of the Indiana University PCPS system (18).

TABLE 2
Positional Parameters and Equivalent Isotropic Displacement Parameters for CsCu$_2$MTe$_4$ (M = Nb, Ta)

Atom	x	y	z	U_{eq}[a]
M = Nb				
Cs(1)	0.29815(6)	0.0141(2)	0.43815(3)	0.01458(12)
Nb(1)	0.29722(13)	0.2595(2)	0.14589(5)	0.0076(2)
Cu(1)	0.03869(13)	0.2680(3)	0.24672(6)	0.0109(2)
Cu(2)	0.2050(2)	0.2589(3)	0.64601(7)	0.0113(3)
Te(1)	0.03452(6)	0.5119(2)	0.14167(3)	0.01021(11)
Te(2)	0.05642(6)	0.5135(3)	0.35074(3)	0.00984(12)
Te(3)	0.28909(6)	0.0005(2)	0.25076(3)	0.00861(12)
Te(4)	0.31148(6)	0.0081(2)	0.04230(3)	0.01204(12)
M = Ta				
Cs(1)	0.2962(4)	0.0130(10)	0.43818(14)	0.0197(6)
Ta(1)	0.2958(3)	0.2594(6)	0.14653(11)	0.0106(4)
Cu(1)	0.0366(7)	0.267(2)	0.2462(3)	0.0140(11)
Cu(2)	0.2057(8)	0.260(3)	0.6457(3)	0.0148(11)
Te(1)	0.0330(3)	0.5111(11)	0.14124(14)	0.0137(6)
Te(2)	0.0542(3)	0.5128(11)	0.3509(2)	0.0129(6)
Te(3)	0.2876(4)	0.0023(12)	0.25075(14)	0.0127(6)
Te(4)	0.3102(4)	0.0098(10)	0.04285(13)	0.0163(6)

[a] U_{eq} is defined as one third of the trace of the orthogonalized U_{ij} tensor.

Structure Determinations

For both compounds initial cell constants and Laue symmetry *mmm* were determined from the analysis of Weissenberg photographs taken at room temperature. Final cell constants were determined from reflections automatically centered at 113 K on a Picker diffractometer (12) in the range 15 < 2θ(MoKα_1) < 46° (43 reflections) for CsCu$_2$NbTe$_4$ and in the range 20 < 2θ(MoKα_1) < 46° (44 reflections) for CsCu$_2$TaTe$_4$. During data collection six standard reflections measured after every 100 reflections showed no significant variations in intensity. The data were processed and corrected for absorption effects with methods and
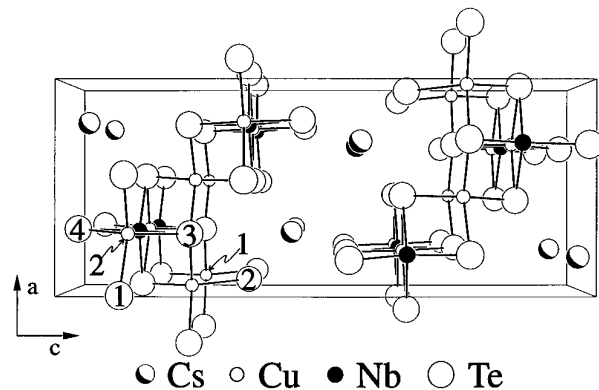

FIG. 1. Unit cell of CsCu$_2$NbTe$_4$. The atom labeling scheme is shown. In this and all subsequent figures, the atoms are drawn with arbitrary size.
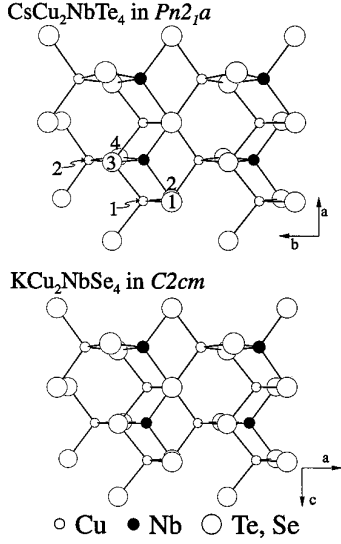
CsCu$_2$NbTe$_4$ in *Pn2$_1$a*

KCu$_2$NbSe$_4$ in *C2cm*

○ Cu ● Nb ◯ Te, Se

FIG. 2. Comparison of a single layer of CsCu$_2$NbTe$_4$ with a layer of KCu$_2$NbSe$_4$ (4). The polar axes for both structures lie within the layers.

programs standard for this laboratory (13). Additional experimental details are given in Table 1.

The systematic absences (0kl, $k + l = 2n + 1$; $hk0$, $h = 2n + 1$) for CsCu$_2$NbTe$_4$ are consistent with the space groups C_{2v}^9-$Pn2_1a$ and D_{2h}^{16}-$Pnma$. The data averaged slightly better in the noncentrosymmetric space group $Pn2_1a$ ($R_{int} = 0.053$) than in the centrosymmetric space group $Pnma$ ($R_{int} = 0.064$). Nevertheless, the space group $Pnma$ was used. The positions of the Cs and Te atoms were determined by direct methods with the program SHELXS (14). The positions of the Cu and Nb atoms were determined from subsequent electron density maps. The structure was refined by full-matrix least-squares techniques with the use of the program SHELXL93 (15), which minimizes the function $\Sigma w(F_o^2 - F_c^2)^2$. Anisotropic displace-
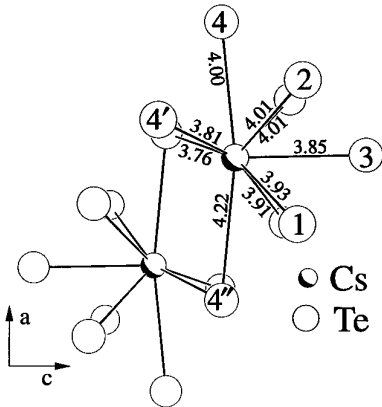

FIG. 3. Coordination of the Cs$^+$ ion in CsCu$_2$NbTe$_4$. Distances are shown in Ångstroms.

TABLE 3
Bond Lengths (Å) and Angles (°) for CsCu$_2$$MTe_4$
(M = Nb, Ta)

	Nb	Ta
Cs(1)–Te(4)#1	3.759(2)	3.776(6)
Cs(1)–Te(4)#2	3.816(2)	3.807(6)
Cs(1)–Te(3)	3.848(1)	3.855(5)
Cs(1)–Te(1)#3	3.915(2)	3.919(7)
Cs(1)–Te(1)#4	3.935(2)	3.937(7)
Cs(1)–Te(4)#5	4.010(1)	4.012(5)
Cs(1)–Te(2)	4.011(2)	4.017(7)
Cs(1)–Te(2)#6	4.016(2)	4.020(7)
Cs(1)–Te(4)#3	4.227(1)	4.242(5)
M(1)–Te(4)	2.608(2)	2.607(6)
M(1)–Te(2)#3	2.614(2)	2.611(6)
M(1)–Te(1)	2.632(2)	2.636(6)
M(1)–Te(3)	2.654(2)	2.640(6)
Cu(1)–Te(2)	2.596(2)	2.612(10)
Cu(1)–Te(3)#5	2.599(2)	2.590(10)
Cu(1)–Te(1)	2.605(2)	2.608(9)
Cu(1)–Te(3)	2.605(2)	2.603(10)
Cu(2)–Te(3)#1	2.592(2)	2.603(14)
Cu(2)–Te(2)#7	2.599(2)	2.601(13)
Cu(2)–Te(1)#2	2.599(2)	2.616(14)
Cu(2)–Te(4)#1	2.603(2)	2.594(13)
M(1)–Cu(1)	2.963(2)	2.956(7)
M(1)–Cu(1)#3	2.963(2)	2.963(7)
M(1)–Cu(2)#8	2.990(2)	3.00(2)
M(1)–Cu(2)#9	2.998(2)	2.99(2)
Te(4)–M(1)–Te(2)#3	108.72(5)	108.24(14)
Te(4)–M(1)–Te(1)	109.95(4)	109.37(13)
Te(2)#3–M(1)–Te(1)	109.38(8)	109.5(3)
Te(4)–M(1)–Te(3)	108.97(8)	109.3(3)
Te(2)#3–M(1)–Te(3)	109.82(4)	110.11(14)
Te(1)–M(1)–Te(3)	109.98(4)	110.27(13)
Te(2)–Cu(1)–Te(3)#5	112.13(5)	111.7(3)
Te(2)–Cu(1)–Te(1)	111.35(7)	111.5(4)
Te(3)#5–Cu(1)–Te(1)	110.59(5)	110.7(2)
Te(2)–Cu(1)–Te(3)	106.14(5)	105.7(2)
Te(3)#5–Cu(1)–Te(3)	103.92(7)	104.6(5)
Te(1)–Cu(1)–Te(3)	112.43(5)	112.4(3)
Te(3)#1–Cu(2)–Te(2)#7	108.04(6)	108.2(3)
Te(3)#1–Cu(2)–Te(1)#2	109.30(6)	109.3(2)
Te(2)#7–Cu(2)–Te(1)#2	110.89(9)	110.5(8)
Te(3)#1–Cu(2)–Te(4)#1	111.06(10)	110.8(8)
Te(2)#7–Cu(2)–Te(4)#1	107.60(6)	108.0(2)
Te(1)#2–Cu(2)–Te(4)#1	109.92(6)	110.0(3)

Note. Symmetry transformations used to generate equivalent atoms: #1 $-x + \frac{1}{2}, y + \frac{1}{2}, z + \frac{1}{2}$; #2 $-x + \frac{1}{2}, y - \frac{1}{2}, z + \frac{1}{2}$; #3 $x + \frac{1}{2}, y, -z + \frac{1}{2}$; #4 $x + \frac{1}{2}, y - 1, -z + \frac{1}{2}$; #5 $x - \frac{1}{2}, y, -z + \frac{1}{2}$; #6 $x, y - 1, z$; #7 $-x, y - \frac{1}{2}, -z + 1$; #8 $-x + \frac{1}{2}, y + \frac{1}{2}, z - \frac{1}{2}$; #9 $-x + \frac{1}{2}, y - \frac{1}{2}, z - \frac{1}{2}$.

ment parameters were refined for all atoms. The resultant agreement indices were $R_w(F_o^2) = 0.221$ and $R_1(F) = 0.076$. In order to obtain reasonable displacement parameters it was necessary to postulate disorder between atoms Nb(1) and Cu(2) and partial occupancy of atom Cu(1). Refine-

TABLE 4
Comparison of Bond Distances for $CsCu_2MTe_4$ (M = Nb, Ta)

Bond	M = Nb	M = Ta	Literature value	Known compound	Reference
M–Te	2.608(2)–2.654(2)		2.690(7)–2.908(7)^a	$NbTe_2$	(19)
		2.607(6)–2.640(6)	2.663(8)–2.923(7)^a	$TaTe_2$	(19)
Cu–Te	2.592(2)–2.605(2)	2.59(1)–2.61(1)	2.583(1)–2.593(1)	$KCuZrTe_3$	(9)
M–Cu	2.963(2)–2.998(2)		2.831(1)–2.833(4)	KCu_2NbSe_4	(4)
		2.956(7)–3.00(2)	2.829(2)–2.831(2)	KCu_2TaSe_4	(5)

^{a} These comparisons are approximate because the M atoms are coordinated to six Te atoms in an octahedral arrangement; there are no known examples of Nb and Ta coordinated to four Te atoms in a tetrahedral arrangement.

ment of an ordered structure in the noncentrosymmetric space group $Pn2_1a$ resulted in reasonable displacement parameters and in a significant improvement in agreement indices, namely $R_w(F_o^2)$ = 0.078 and $R_1(F)$ ($F_o^2 > 2\sigma$ (F_o^2)) = 0.036. This model included a secondary extinction coefficient. The final difference electron density map shows no features with heights greater than 0.6% that of a Te atom.

The structure solution for $CsCu_2NbTe_4$ was used in the initial refinements of $CsCu_2TaTe_4$. Refinement in space group $Pn2_1a$ paralleled that from the Nb structure. There were mechanical troubles with the diffractometer during data collection; it is therefore not surprising that the data for this structure are poor, with R_{int} = 0.154. Nevertheless, the essential features of the structure remain clear. The final agreement indices are $R_w(F_o^2)$ = 0.231 and $R_1(F)$ = 0.102. The final difference electron density map shows no features with heights greater than 5.2% that of a Te atom.

Final values of atomic parameters and equivalent isotropic displacement parameters are given in Table 2 for $CsCu_2NbTe_4$ and $CsCu_2TaTe_4$. Final structure amplitudes, anisotropic displacement parameters, and a complete listing of bond distances and angles are available as supplementary material.[1]

RESULTS AND DISCUSSION

The compounds $CsCu_2MTe_4$ (M = Nb, Ta), to our knowledge, are the first tellurides to be reported in the growing family of ACu_2MQ_4 compounds. These two-dimensional materials contain $^2_\infty[Cu_2MTe_4^-]$ layers separated by Cs^+ cations. The unit cell of $CsCu_2NbTe_4$ is shown in

Fig. 1. Similar copper–metal–chalcogen layers were found previously in the compounds KCu_2MSe_4 (M = Nb (4), Ta (5)). The differences between the structures of the current Cs/Te compounds and the similar K/Se compounds are found in the positions of the $^2_\infty[Cu_2MQ_4^-]$ (Q = Se, Te) layers relative to one another. In KCu_2MSe_4, the layers are eclipsed and the compounds crystallize in a C-centered orthorhombic lattice; in $CsCu_2MTe_4$ the layers are slightly slipped along [100] and the compounds crystallize in a primitive lattice. Both sets of compounds are noncentrosymmetric and the polar axes in both lie along the layers (Fig. 2).

The Cs^+ cations in $CsCu_2NbTe_4$ are coordinated to nine Te atoms in a highly distorted tricapped trigonal prism (Fig. 3 and Table 3). Eight of the Cs–Te interactions fall in the range 3.759(2)–4.016(2) Å and agree well with those found in $CsCuUTe_3$ (16) (3.740(2) to 4.040(1) Å). The ninth is a longer distance at 4.227(1) Å. The K^+ ion found between the layers of KCu_2MSe_4 (M = Nb, Ta) exhibits a more regular tricapped trigonal prismatic geometry.

Within the $^2_\infty[Cu_2MTe_4^-]$ layers, the Cu and M atoms are tetrahedrally coordinated to four Te atoms. The two unique $CuTe_4$ and one MTe_4 tetrahedra are interconnected so that edge sharing occurs only between Cu- and M-centered polyhedra; $Cu(1)Te_4$ and $Cu(2)Te_4$ tetrahedra only share corners. The connectivity of these tetrahedra found in $CsCu_2NbTe_4$ is shown in Fig. 2. Bond distances for both compounds agree well with those in known compounds, as shown in Table 4. As expected, the M–Cu distances in the present Te compounds are slightly longer than those found in the similar Se compounds. The Te–M–Te angles for $M(1)$ and Cu(2) are close to the ideal tetrahedral value (107.60(6) to 111.06(10)° for M = Nb, 108.0(2) to 110.11(14)° for M = Ta). The tetrahedron surrounding the Cu(1) atom is slightly distorted with angles of 103.92(7) to 112.43(5)° for M = Nb and 104.6(5) to 112.4(3)° for M = Ta.

The shortest Te ⋅⋅⋅ Te distances are 3.923(1) and 3.937(4) Å in $CsCu_2NbTe_4$ and $CsCu_2TaTe_4$, respectively, and hence formal oxidation states of Te(−II), Cs(I), Cu(I),

and Nb(V) may be assigned. Such an assignment is consistent with the highly resistive nature of these compounds. Room-temperature two-probe electrical conductivity measurements of CsCu$_2$$MTe_4$ (M = Nb, Ta) show conductivities that are less than 2.5(5) $\times$ 10^{-5} Ω^{-1} cm^{-1} and 2.2(1) $\times$ 10^{-4} Ω^{-1} cm^{-1} for M = Nb and Ta, respectively.

REFERENCES

1. M. Latroche and J. A. Ibers, *Inorg. Chem.* **29,** 1503 (1990).
2. Y.-J. Lu and J. A. Ibers, *Inorg. Chem.* **30,** 3317 (1991).
3. Y.-J. Lu, P. Wu, and J. A. Ibers, *Eur. J. Solid State Inorg. Chem.* **30,** 101 (1993).
4. Y.-J. Lu and J. A. Ibers, *J. Solid State Chem.* **94,** 381 (1991).
5. Y.-J. Lu and J. A. Ibers, *J. Solid State Chem.* **107,** 58 (1993).
6. J. A. Ibers and Y.-J. Lu, *J. Solid State Chem.* **111,** 447 (1994).
7. Y.-J. Lu and J. A. Ibers, *Comments Inorg. Chem.* **14,** 229 (1993).
8. M. F. Mansuetto, P. M. Keane, and J. A. Ibers, *J. Solid State Chem.* **105,** 580 (1993).
9. M. F. Mansuetto, P. M. Keane, and J. A. Ibers, *J. Solid State Chem.* **101,** 257 (1992).
10. J. A. Cody and J. A. Ibers, *Inorg. Chem.* **33,** 2713 (1994).
11. P. M. Keane and J. A. Ibers, *Inorg. Chem.* **30,** 1327 (1991).
12. J. C. Huffman, Ph.D. Thesis, Indiana University, 1974.
13. J. M. Waters and J. A. Ibers, *Inorg. Chem.* **16,** 3273 (1977).
14. G. M. Sheldrick, SHELXTL PC Version 5.0, An Integrated System for Solving, Refining, and Displaying Crystal Structures from Diffraction Data. Siemens Analytical X-Ray Instruments, Inc. Madison, WI, 1994.
15. G. M. Sheldrick, *J. Appl. Crystallogr.*, in press (1995).
16. J. A. Cody and J. A. Ibers, *Inorg. Chem.* **34,** 3165 (1995).
17. J. de Meulenaer and H. Tompa, *Acta Crystallogr.* **19,** 1014 (1965).
18. J. C. Huffman and W. E. Streib, Unpublished work, 1990.
19. B. E. Brown, *Acta Crystallogr.* **20,** 264 (1966).